Article

Journal of Advanced Electrochemical Storage

www.pubj.org

J. Adv. Electro. Storage Vol.no.1, Issue no.2, July-December, 2025, 107–115

Temperature dependents struct-optical properties of spinel type $FeCr_2O_4$ by glycine mediated combustion method

Tholkappiyan Ramachandran[1*]

[1,*] Department of Physics, College of Science, United Arab Emirates University, Al-Ain, Abu Dhabi, P. O. Box 15551, United Arab Emirates.

*Corresponding author: thols2006@gmail.com

ABSTRACT: Nanocrystalline spinel type FeCr2O4 samples were prepared by glycine mediated combustion method and the obtained samples were annealed at different temperature ranging from 300–700°C for constant interval of 6 h. The annealed FeCr2O4 samples were characterized by X-ray diffraction (XRD), Fourier transform infrared (FTIR) spectroscopy methods. The morphology was examined using a scanning electron microscopy (SEM) and corresponding presence of elements and homogeneous distribution were observed from EDS mapping. The XRD results reveal that the XRD diffraction peaks of the annealed FeCr2O4 were of well crystalline and correspond to the cubic crystal system. Morever, the confirmation for absence of secondary phases in the annealed samples were determined from XRD and FTIR results. The SEM result confirms the porous structure with spongy network of as-synthesized sample and after annealed, porosity content of FeCr2O4 samples were get reduced with enhance the agglomeration. EDS analysis confirms the presence of elements in the FeCr2O4 samples and corresponding homogeneous distribution of these elements were showed in EDS mapping. The crystallite size, lattice strain, lattice deformation stress and deformation energy density for annealed (300–700°C) FeCr2O4 samples were determined by three different models such as Uniform Deformation model (UDM), Uniform stress deformation model (USDM) and Uniform deformation energy density model (UDEDM) based on Williamson–Hall (W–H) plot from powder X-ray diffraction data. The results of estimated average crystallite size of annealed FeCr2O4 samples by Scherrer and W–H plot methods were compared with SEM results. It is found that the average crystallite size measured by W–H plot methods is in good agreement with Scherrer results.

Keywords: Spinel; FeCr2O4 nanoparticles; glycine mediated combustion method; temperature; X−ray diffraction.

1. Introduction

Iron chromite (FeCr2O4), often known as normal spinel in spinel groups, is an important and promising material owing to their many typical properties such as cubic structure, transparency in the visible range, direct or indirect wide band gap and applied in practical applications in hydrogen generation under visible irradiation and photocatalysts [1]. Iron chromite with chemical formula of A2+B23+O4, where A-site contains Fe2+ ion that occupied in tetrahedral site with electronic configuration of 3d6 and whereas the B-site contains Cr3+ that occupied in octahedral site with electronic configuration of 3d3. Depending upon the temperature, the crystal structure of iron chromite, FeCr2O4 will be: at room temperature the cubic phase is stable, whilst at about 135.15 K it transforms into a tetragonal phase and at about

70.15 K into an orthorhombic phase [2]. The room temperature crystal structure of iron chromite, FeCr2O4 has cubic symmetry with a space group of Fd-3m having lattice constant of a = 8.378 Å and the oxygen parameter of u = 0.3861 [3] respectively

In this present work we aim at synthesizing nanocrystalline iron chromite, FeCr2O4 and evaluating micro-structural parameters such as crystallite size, lattice strain, texture coefficient, dislocation density, lattice stress, unit cell volume, lattice constants, X-ray density, specific surface are etc. including morphological and optical characteristics of spinel type nanocrystalline iron chromite, FeCr2O4. And, also studied the change in the micro-strucutural properties by varying the temperature in the range of 300−700°C. A series of characterization techniques such as X−ray diffraction (XRD), Fourier transform infrared spectroscopy (FTIR), Scanning electron microscopy (SEM), Energy dispersive X−ray (EDS) and UV/Vis/NIR spectroscopy were employed to study the micro-structural properties and the morphologies of the prepared FeCr2O4 samples. In addition, we also carried out a comparative study of average crystallite size and lattice strain by employing the Scherrer plot, modified form of the Williamson–Hall (W–H) method, namely uniform deformation model (UDM), uniform stress deformation model (USDM) and uniform deformation energy–density model (UDEDM)

2. Experimental

2.1 Materials and sample preparation

The starting metal nitrates: Iron (III) nitrate nonahydrate (FeN3O9·9H2O, ≥98%), chromium (III) nitrate nonahydrate (CrN3O9·9H2O, 99%) and fuel: glycine (C2H5NO2, ≥98.5%) were purchased from sigma-aldrich. The AR-grade materials were used in the sample preparation without further purification. The deionized water was used throughout the chemical combustion synthesis reaction.

Spinel type nanocrystalline FeCr2O4 samples were prepared by combustion method. The stoichiometric amounts of metal nitrates were dissolved in 40 ml of deionized water to obtain the starting nitrate solutions. The above materials were mixed according to the chemical ratio of 1:2:4 for FeCr2O4. Then, the solution was added with 5 ml of Conc. HNO3 and stirred for 30 min to become a clear homogeneous solution. To this aqueous solution of fuel was added and vigorous stirred at 80°C for 2 h. Then, the temperature was raised to 200 °C and kept at this temperature until the sol turned into a dark viscous gel. The gel was then heated to 300 °C for 25 min leading to the gel ignited and burnt with glowing flints and to produce the large amount of gaseous products. The self-ignition and end of the chemical reaction time interval was >20 s. To allow complete combustion, the temperature was further heat treated for 20 mins. The resultant powders with extremely fine, porous and foamlike structure was obtained. The synthesized powders were annealed at different temperature ranging from 300–700°C for constant interval of 6 h and stored it further characterizations. The schematic scheme of synthesized iron chromite, FeCr2O4 nanoparticles were prepared via combustion method with different annealed temperatures is shown in figure 1.

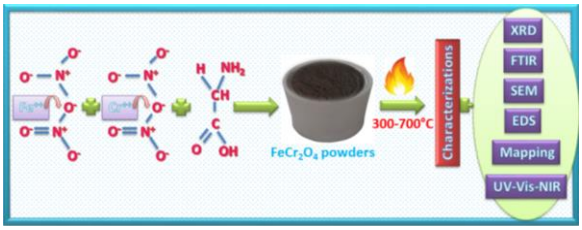

Figure 1. Schematic representation of samples prepared by glycine mediated combustion method.

2.2. Characterization

The structural analysis of synthesized powders were recorded by Powder X–ray

diffraction measurements using SHIMADZU Lab X–XRD–6100 Powder X-ray diffractometer unit operated at 298 K using Cu-Kα radiation in the 2θ range of 10° to 120° with step size of 0.02°/min. Phase identification of samples was carried out using powder database PDF-4+ of the International Center for Diffraction Data (ICDD). For FT-IR spectrum of all synthesized samples were recorded using a VARIAN 3100, Excalibur series FT-IR Spectrophotometer. Samples were prepared by diluting the sample powders with potassium bromide (KBr, BDH Chemicals Ltd, Poole, England) and then pressed into a disc (1 mm thickness). The FTIR spectra were recorded in the range from 400 to 4000 cm–1 using VARIAN software at room temperature. The surface morphology and presence of elements in the synthesized samples was examined using JEOL JSM–6010LA scanning electron microscopy (SEM) which is operated at 20 keV accelerating voltage. The Images were obtained in secondary electron imaging (SEI) mode. Elemental mapping were performed with energy–dispersive X–ray spectroscopy (EDS). The optical spectrum were measured by Jasco V–670 spectrophotometer over a UV/Vis/NIR region in the diffuse reflectance mode. Samples were prepared by completely dissolved into solvent to form a transparent solutions. UV/Vis/NIR spectra were collected from these transparent solutions. The light sources used are a deuterium (D2) lamp for the UV region and a halogen (WI) lamp for the VIS/NIR region.

3. Results and discussion

3.1. X–ray diffraction studies

The structure and phase purity of the FeCr2O4 samples annealed at different temperature were confirmed by analyzing the X-ray powder diffraction patterns. Fig. 2 shows the powder XRD patterns of the FeCr2O4 samples annealed at different temperature via glycine mediated combustion method. The peaks in the XRD pattern could be indexed with the hkl values of (111), (220), (311), (222), (400), (331), (422), (511), (440), (620), (533), (444), (711), (642), (731), (800), (751), (840) and (911) which are characteristics of single-phase cubic spinel structure (JCPDS card no. 04−006−2807) belonging to the Fd-3m space group. There is no additional peak for all annealed samples, which indicates that all the FeCr2O4 samples crystallize in single-phase cubic spinel structure [26]. Further, it suggesting that pure products were obtained by glycine mediated combustion method. Fig. 1 shows the higher magnification images of powder XRD pattern of synthesized FeCr2O4 samples. As it seen in Fig. 1, it was concluded that (1) intensity and (2) shift are the two important factors that affects the crystal structure of synthesized FeCr2O4 samples by influence of temperatures. For (1), the gradual increase in intensity of diffraction peaks with increase in temperatures are due to improving crystallinity of the materials. Whereas for (2), with the temperature increasing, there was a zigzag shift in 2θ angle, indicating irregularities in the crystal structure can cause lattice strains. Thus clearly confirmed that temperature have greatly affected in the crystal lattice of synthesized FeCr2O4 samples [14]. The obvious increase in XRD intensity suggests that the (hkl) orientation gets stronger continuously with increasing crystalline size. In the present work, we used texture coefficient (Tc) for quantify the preferential orientation of (hkl) plane in the materials. The texture coefficient of each (hkl) plane in the XRD pattern of synthesized FeCr2O4 samples is determined using the following formula [23],

$$TC = \frac{I_{(hkl)}/I_{0_{(hkl)}}}{1/N\,(\Sigma I_{(hkl)}/I_{0_{(hkl)}})} \quad (1)$$

Where TC is the texture coefficient, I(hkl) is the measured XRD intensity of plane (hkl), n is the number of reflection in the diffraction peaks and Io(hkl) is the reference XRD intensity of the plane (hkl) taken from the JCPDS card

(04−006−2807) data. From the above equation, TC(hkl)≈1 for all the (hkl) planes considered, then the powder samples are with a randomly oriented crystallite similar to the JCPDS reference, while values higher than 1 (TC(hkl)>1) indicate the preferentially oriented of grains in a given (hkl) direction and values (TC(hkl)<1) indicate the lack of grains oriented in that (hkl) direction. The obtained averages TC from Eqn. (9) for synthesized with different heat temperatures of FeCr2O4 samples. These results suggest that the higher values of TC preferred orientation is associated with the increased number of grains along with the respective (hkl) planes [21, 22]. Further, it is suggest that the increased in temperature of synthesized FeCr2O4 samples with increase the TC along the different planes for FeCr2O4 samples.

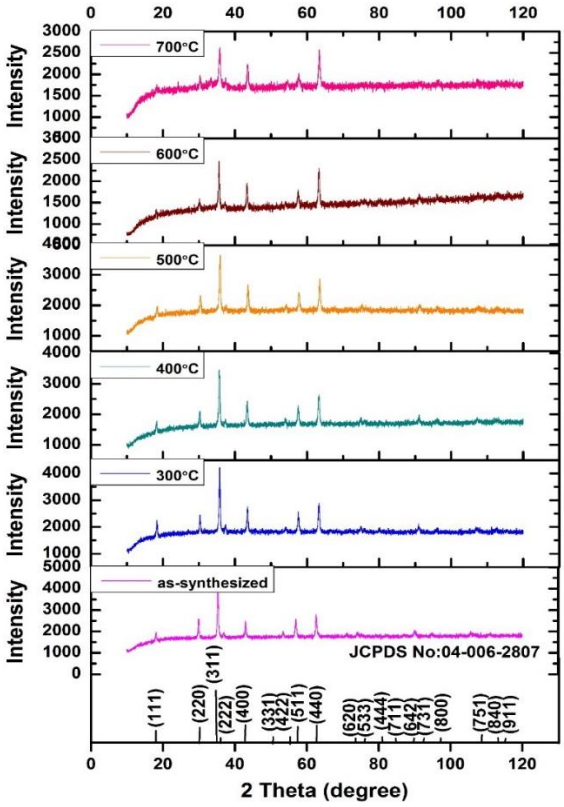

Fig. 2 X–Ray diffraction patterns of synthesized FeCr2O4 samples annealed at different temperature via glycine mediated combustion method.

3.1.1. Williamson-Hall (W–H) method

3.1.1.1 Determination of lattice strain using Uniform Deformation model (UDM)

In order to better understanding the peak shift for the synthesized FeCr2O4 samples by different heat treatment, we suggested Williamson–Hall (W–H) model. W–H analysis is a simplified integral breadth method where both grain size and lattice strain induced broadening are deconvoluted by considering the peak width as a function of 2θ angle.

$$\beta hkl = \beta(\text{grain size}) + \beta(\text{strain}) \quad (2)$$

Hence, total peak broadening, W–H equation can be expressed by an equation [13],

$$\frac{\beta hkl}{\cos\theta} = 4\varepsilon \sin\theta + K\lambda/Lavg \quad (3)$$

Where ε is the lattice strain, K is a constant equal 0.9, βhkl is the peak width at half maximum (FWHM) intensity, λ is the wavelength of X−ray radiation, Lavg is the average grain size and θ is the peak position. W–H plots for synthesized FeCr2O4 samples were obtained by plotting with 4 sin(θ) in x-axis and βhkl cos(θ) in the y-axis as shown in Fig. 3. Less scattering of data points in the W–H plots for all the samples indicates the homogeneous of size distribution as well as low values of lattice strain (ε). By applying the best linear fit of the data, W–H plot shows a straight line in which the slope gives the value of lattice strain (ε) and the reciprocal of the intercept determines the average grain size (Lavg). The calculated values of lattice strain and average grain size are mentioned in Fig. 4. The average grain size (Lavg) estimated from the Williamson–Hall (W–H) model increased with the increased heat treatment in the synthesized FeCr2O4 samples. In contrast, the lattice strain increased and the value of strains in heat treated samples was much higher than that in un-treated FeCr2O4 samples. Alternatively, the lattice parameter (a) of the synthesized FeCr2O4 samples slightly decreased with an increase of the heat treatment as mentioned below. Hence, the lattice shrinkage in this present

study should be caused by a compression effect from the heat treatment using the glycine mediated combustion method. However, this tendency was observed in an earlier report by many researchers on nanocrystalline spinel ferrites [31,32].

Fig. 3 Higher magnification images of powder XRD pattern of synthesized FeCr2O4 samples prepared by glycine mediated combustion method.

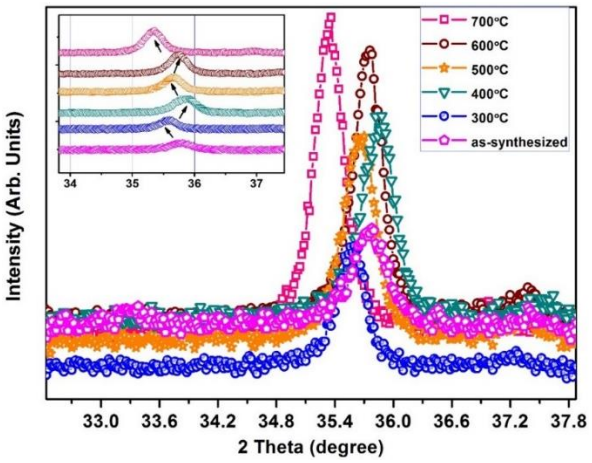

Fig. 4 Williamson–Hall plots of (a) as-synthesized, (b) 300°C, (c) 400°C, (d) 500°C, (e) 600°C and (f) 700°C of annealed FeCr2O4 samples via glycine mediated combustion method.

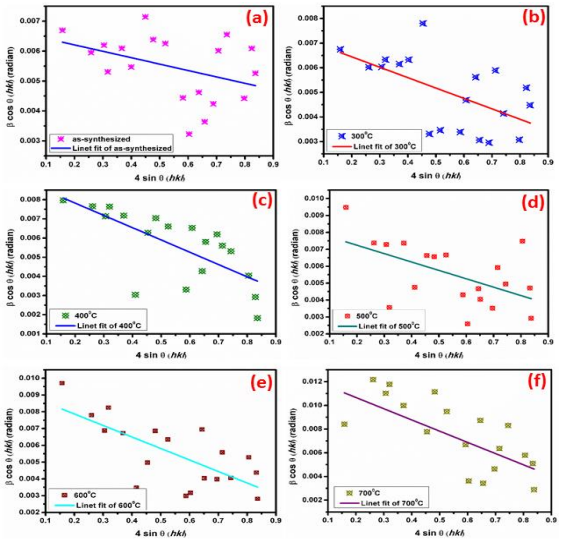

Fig. 5 (a-f) Uniform stress deformation model (USDM) fitting of XRD data for FeCr2O4 samples obtained different temperatures. The experimental data are shown with symbols and fitted data are shown with solid line.

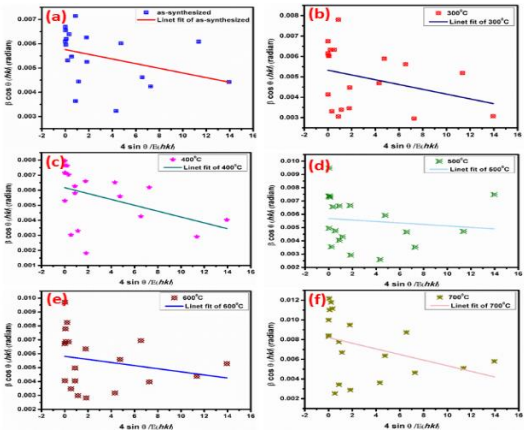

Fig. 6 (a-f) Uniform deformation energy density model (UDEDM) fitting of XRD data for FeCr2O4 samples obtained different temperatures. The experimental data are shown with symbols and fitted data are shown with solid line.

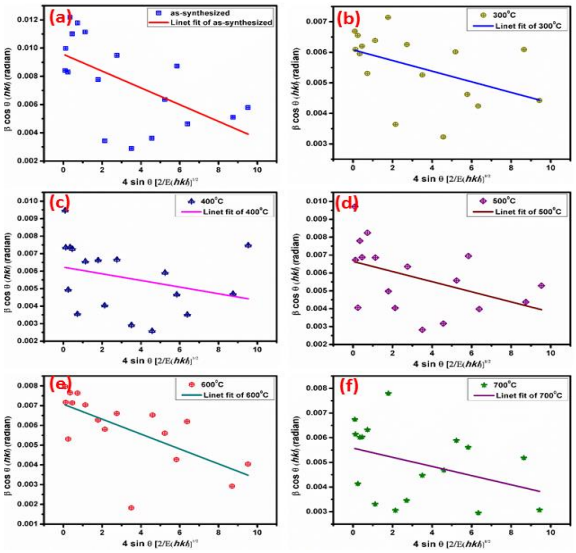

3.1.1.2. Estimation of lattice deformation stress (s) and crystallite size (Lavg) by Uniform stress deformation model (USDM)

Here lattice deformation stress, crystallite size and lattice strain are the other main factors were taken into consideration the

anisotropic in nature of Young's modulus Uniform stress deformation model (USDM) assumes that the crystal is anisotropic in nature of Young's modulus of the crystal is more realistic. Assuming a lattice strain to be present in the annealed FeCr2O4 samples, Hook's law can be applied to estimate the lattice deformation stress to a reasonable approximation. Hence, we consider Hook's law. The stress is directly proportional to the strain, with a proportionality constant which is Young's modulus (E) and is given by s=Eε where E is the Young's modulus or modulus of elasticity, s and ε is the stress and strain in the crystal. By substituting the value of ε in Eq. (5) will be getting the modified Williamson-Hall equation and can be expressed as [29]:

$$\beta hkl \cos \theta = 4(s/Ehkl)\sin \theta + K\lambda/Lavg \quad (4)$$

where Ehkl is Young's modulus in the direction perpendicular to the set of the crystal plane (hkl). For a given cubic crystal, Young's modulus is given by the following relation [45].

$$1/Ehkl = S11 - 2[(S11 - S12) - \tfrac{1}{2} S44](l2m2 + m2n 2 + n2l2) \quad (5)$$

Where S11, S12, S44 are the elastic compliances of spinel FeCr2O4 samples and l, m, n are the cosines of the angles between the direction to which Ehkl is referred and the crystal axes. The relations which provide the connection between the elastic compliances (S11, S12, S44) and the elastic stiffness Ci j are as follows:

$$C44 = 1/S44,$$
$$C11 - C12 = 1/(S11 - S12),$$
$$C11 + 2C12 = 1/(S11 + 2S12) \quad (6)$$

The values of elastic stiffness C11, C12, C44 for spinel chromate are 275 GPa, 104 GPa, 95.5 GPa respectively [15]. The Ehkl value for cubic spinel FeCr2O4 samples was calculated as 2.44 TPa. Fig. 5 shows the plot of βhkl cos θ against 4sin θ/(Ehkl) for all the peaks in a FeCr2O4 sample and this process was repeated for annealing samples. From the figure experimental data points are shown with symbols and the fitted data points are shown with straight line. The slope and the intercept of the figure both the uniform stress (s) and the crystallite size (Lavg) were obtained. Then, we can calculate the strain from the linear relation between stress and strain s =εY. In this model, the lattice strain again increases with increasing annealing temperatures of FeCr2O4 samples. Similarly, average crystallite size systematically increases with increasing annealing temperatures. And also note that the crystallite size obtained in this model is quite close to that obtained from the UDM model, while the strain values are quite different in these two models.

3.1.1.3. Estimation of lattice deformation stress (s) and energy density (U) by Uniform deformation energy density model (UDEDM)

In order to determine the deformation energy density, crystallite size, stress and strain parameters, we suggested Uniform deformation energy density model (UDEDM) assumes that the crystal are homogeneous and isotropic in nature. However, in many cases, the assumption is not fulfilled. Moreover, all the constants proportionality associated with the stress–strain relation are no longer independent when the lattice strain energy density (u) is considered. According to Hook's law of elastic system, the energy per unit volume (energy density, u) can be calculated from u= (Ɛ2*Ehkl) /2, and therefore, the modified equation can be expressed as,

$$\beta hkl \cos \theta = 4\sin \theta (2u/Ehkl)1/2 + K\lambda/Lavg \quad (4)$$

Eq. (6) represents the UDEDM. Fig. 5 shows the plots between the βhkl cos θ and 4sin θ (2/ Ehkl)1/2 for all the peaks in a FeCr2O4 sample and this process was repeated for annealing samples. The experimental data points are shown with symbols and the fitted data is shown with a straight line. The energy density, u is estimated from the slope and the crystallite size is estimated from the y-intersection of the linear fit made to the graph. Using the relation s =ε*Ehkl

and u = s2/(2*Ehkl) we can calculate the stress and strain on the FeCr2O4 sample. The calculated parameters like crystallite size, lattice strain, lattice deformation stress and deformation energy density values from this model. This method also concludes that the crystallite size increases with increasing annealing temperatures of FeCr2O4 samples. The lattice strain values obtained for these samples using the above models (USDM and UDEDM) are fully consistent.

3.1.2. Scherrer method

In order to compare the average grain size of synthesized FeCr2O4 samples, we suggested usual Scherrer method. The average grain size of the FeCr2O4 samples annealed at different temperature is calculated from the maximum diffraction peak of the (311) plane in the XRD profile, in accordance with Scherrer formula [10],

$$Lavg = 0.89\,\lambda / (\beta \text{ corrected } \cos\theta) \quad (8)$$

Where Lavg is the average crystallite size, λ is the wavelength of X-ray radiation (0.1542 nm), β is the full width at half maximum (311) peak and θ is the Bragg's angle. The calculated average grain sizes obtained from the Scherrer method by using XRD data for synthesized FeCr2O4 samples are listed in Fig. 5. It shows that average grain sizes are slight vary in comparison to Williamson–Hall (W–H) model. This is because of lattice strains are induced in the synthesized FeCr2O4 samples by increasing the applied temperatures. If compared to previous literature, obtained values are good agreement with 47 nm for FeCr2O4 by nitrates decomposition [1], 30.2 nm for MgCr2O4 by sol-gel method [12] and 28.7 nm for Mg1–xZnxFeCrO4 by conventional solid phase reaction [11], respectively. Moreover, the values of average grains for FeCr2O4 samples are increased with raising the temperature from 300-700°C; which is due to grain growth happens where the smaller grains are coalescence into larger grains by solid-state diffusion which, in turn, reduces the free energy in the system by reducing the surface area. Since the more diffusion is happen at elevated temperatures, larger grains were obtained at higher annealing temperatures [29]. The similar types of results were reported earlier by many researchers for the polycrystalline spinel ferrites synthesized by the different chemical methods [34, 35]. Therefore the grain size of FeCr2O4 samples can be greatly tuned by applying the temperatures without changing the preparation conditions.

The amount of defects in the synthesized FeCr2O4 samples can be expressed in term of the dislocation density (δ), that known as the length of dislocation per unit volume in the crystal. The dislocation density (δ) of the synthesized FeCr2O4 samples can be expressed as [],

$$\delta = 1/(Lavg)2 \quad (12)$$

where Lavg is the average crystallite size. It is known that, the calculated value of dislocation density is attributed to the amount of defects in a crystal of FeCr2O4 samples. The dislocation density as a function of different annealed temperature of the FeCr2O4 samples were estimated. The decreased values of dislocation density reveal that, the δ values were affected by the annealed temperature. This result showed that the formed phase is partially crystalline so the line defects are easily occurred on the surface.

The number of unit cells (n) of the FeCr2O4 samples was calculated using the following formula [27,28],

$$n = 3.14*D3 / 6(V) \quad (7)$$

where V is the volume of unit cell. The calculated values of unit cell (n) for FeCr2O4 samples at a different annealed temperature. It is observed that, the number of crystallite size per unit volume is increased by increasing the annealed temperature of FeCr2O4 samples. This is due of the observed increase in the average grain sizes of FeCr2O4 samples which leads to increase the crystal growth and decrease the defects in crystallites.

The lattice constant of synthesized FeCr2O4 samples was calculated using the expression [],

1/d2= (h2+k2 +l2)/a2 (13)

Where 'd' is the interplanar spacing, 'a' is the lattice constant in angstrom (Å) and (hkl) are the Miller indices of prominent peak in the XRD pattern. The calculated values of lattice constant as a function of temperature is found to be in the range of 8.362–8.271 Å. It can be seen that the lattice constant of synthesized FeCr2O4 samples decreases with increasing in the temperatures. The decrease of lattice constant 'a' can be explained on the basis of applied temperature effect, lattice strain and redistribution of cations on A-site (Fe) and B-site (Cr) in the FeCr2O4 [14, 31, 32]. Moreover, these values are agreed well with previous literature of 8.371 Å for FeCr2O4 by A. Boudjemaa et. al. [1].

In addition, the theoretical X−ray density (dX) for synthesized FeCr2O4 samples at different temperatures was calculated using the following formula,

dX=ZM/Na3
(14)

Where Z is the number of molecules per unit cell (Z=8) for the prepared spinel FeCr2O4 samples, N is the Avogadro's number=6.023x1023, M is the molecular weight, and 'a' is the lattice constant in angstrom (Å). The X-ray density was found to be in the range of 5.08–5.25 g/cm3 depending upon the heat treatment temperature. All of these values are in good agreement to the earlier reported values for this structure [33]. Increasing behavior of dX are expected due to decreasing the values of lattice constant of the FeCr2O4 samples.

Further, specific surface area (S) of synthesized FeCr2O4 samples at different temperatures can be calculated using the following expression,

S=6/dX(Lavg)
(15)

The value of obtained specific surface area for samples FeCr2O4 are found in the range of 25.78–19.30 m2/g respectively. It shows that S values are decreased due to increasing the values of average grain size in the FeCr2O4 samples.

4. CONCLUSIONS

In conclusion, we report the influence of the temperature effect on the micro-structural properties of nanocrystalline spinel type FeCr2O4. In this study X-ray diffraction line profile analysis was employed to investigate the strain effect of the nanocrystalline FeCr2O4 while controlling particle sizes from 43.7 to 58.2 nm. The observations reveal a negative strain which indicates the relaxive in FeCr2O4. The intensity ratio of the I/Imax modes exhibits strong size dependence. As the particle sizes increase further, the ratio increases moderately.

Conflicts of interest

There are no conflicts to declare.

References

1. M. Birkholz, Thin Film Analysis by X-Ray Scattering, Wiley-VCH Verlag GmbH & Co. KGaA, Weinheim, 2006.
2. T. Prasada Rao, M.C. Santhoshkumar, Appl. Surf. Sci. 255 (2009) 7212–7215.
3. A. Boudjemaa, R. Bouarab, S. Saadi, A. Bouguelia, M. Trari, Photoelectrochemical H2-generation over Spinel FeCr2O4 in X2 solutions(X2¬¬ = S2 and SO2 3), Applied Energy 86 (2009) 1080–1086. doi:10.1016/j.apenergy.2008.06.007
4. K. A. M. Khalaf , A. D. Al-Rawas, H. M. Widatallah, K. S. Al-Rashdi, A. Sellai, A. M. Gismelseed, Mohd Hashim, S. K. Jameel, M. S. Al-Ruqeishi, K. O. Al-Riyami, M. Shongwe, A. H. Al-Rajhi Influence of Zn2+ ions on the structural and electrical

properties of Mg1–xZnxFeCrO4 spinels, Journal of Alloys and Compounds 657 (2016) 733–747.
5. Haiyan He, Catalysis and Photocatalysis of MgCr2O4 Powder at Room Temperature, Recent Patents on Chemical Engineering, 2010, 3, 74–77.
6. S. Ayyappan, G. Gnanaprakash, G. Panneerselvam, M. P. Antony, J. Philip, J. Phys. Chem. C112 (2008) 18376.
7. R.N. Panda, J. C. Shih, T. S. Chin, J. Magn. Magn. Mater. 257 (2003) 79–86.
8. L. Ben Taha, M.Artus, S. Ammar, L. S. Smiri, F. Herbst, M. J. Vaulay, V. Richard, J. M. Greneche, F. Villain, F. Fievet, J. Magn. Magn. Mater. 320 (2008) 3242–3250.
9. V. Senthilkumar, P. Vickraman, J.J. Prince, M. Jayachandran, C. Sanjeeviraja, Effects of annealing temperature on structural, optical, and electrical properties of antimony-doped tin oxide thin films, Philos. Mag. Lett. 90 (2010) 337e347.
10. N. Rezlescu, E. Rezlescu, J. Phys. IV 07 (1997) 225–226.
11. Liping Guo, Xiangqian Shen, Xianfeng Meng, Yuhua Feng, J. Alloy. Compd. 490 (2010) 301–306.
12. Kwang Pyo Chae, Young Bae Lee, Jae Gwang Lee, Sung Ho Lee, J. Magn. Magn. Mater. 220(2000)59–64.